

# YARE-GAN: Yet Another Resting State EEG-GAN

**Yeganeh Farahzadi**

Institute of Psychology, ELTE Eötvös Loránd University  
Budapest, 1064, Hungary

**Morteza Ansarinia**

University of Luxembourg  
Belval, Luxembourg

**Zoltán Kekecs**

Institute of Psychology, ELTE Eötvös Loránd University  
Budapest, 1064, Hungary

## Abstract

**Generative Adversarial Networks (GANs) have shown promise in synthesizing realistic neural data, yet their potential for unsupervised representation learning in resting-state EEG remains underexplored. In this study, we implement a Wasserstein GAN with Gradient Penalty (WGAN-GP) to generate multi-channel resting-state EEG data and assess the quality of the synthesized signals through both visual and feature-based evaluations. Our results indicate that the model effectively captures the statistical and spectral characteristics of real EEG data, although challenges remain in replicating high-frequency oscillations in the frontal region. Additionally, we demonstrate that the Critic's learned representations can be fine-tuned for age group classification, achieving an out-of-sample accuracy, significantly better than a shuffled-label baseline. These findings suggest that generative models can serve not only as EEG data generators but also as unsupervised feature extractors, reducing the need for manual feature engineering. This study highlights the potential of GAN-based unsupervised learning for EEG analysis, suggesting avenues for more data-efficient deep learning applications in neuroscience.**

**Keywords:** Generative adversarial networks (GANs); EEG; Unsupervised Representation Learning

## Introduction

Generative AI—including techniques such as Generative Adversarial Networks (GANs) (Goodfellow et al. (2014)), Variational Autoencoders (VAEs) (Kingma (2013)), and diffusion models (Ho et al. (2020))—is being increasingly recognized as a powerful tool in neuroscience. It has found various applications ranging from synthesizing neural data to also learning reusable representations of neural signals in an unsupervised manner.

One of the challenges in neuroscience is the limited availability of high-quality neural data, as collecting such data is often costly and time-consuming. Generative AI can help address this issue by creating realistic synthetic datasets that capture the statistical properties of real neural recordings. Additionally, in cases where labeled data is sparse or certain

conditions are underrepresented, synthetic data can help balance datasets, leading to more robust analyses and improved model performance (Murphy (2022)). The use of generative AI—particularly GANs—for data augmentation in neural datasets has been relatively well studied. Prior research has demonstrated that augmenting datasets with generated neural signals can enhance classification accuracy in tasks such as motor imagery (Hartmann et al. (2018); Fahimi et al. (2020)), emotion recognition (Pan & Zheng (2021)), and detection of epileptic seizure (Pascual et al. (2020)).

Beyond data augmentation, generative AI—particularly GANs—also provides a way to learn meaningful feature representations in an unsupervised manner (Radford (2015)). By learning a latent space that effectively captures the underlying structure of neural data, GANs can generate interpolated samples that preserve key statistical and physiological properties. These learned representations can be repurposed for supervised tasks, reducing the need for extensive and often labor-intensive feature engineering. This approach is particularly beneficial for neural signal processing, where preprocessing and manual feature extraction can significantly influence final results (Robbins et al. (2020); Botvinik-Nezer et al. (2020)). This way, an unsupervised generative model can first be trained using publicly available, large-scale resting-state datasets and later fine-tuned on task-specific data, which is often more limited. In this way, generative AI not only mitigates the issue of limited case-specific samples through data augmentation but also tackles this issue by offering transferable, reusable representation of the data that can later be fine-tuned for a downstream, case-specific supervised task.

While deep learning approaches for unsupervised representation learning in neuroscience have primarily relied on AutoEncoder-based architectures Wang et al. (2024), the use of GANs for this purpose remains relatively underexplored, with some studies investigating their potential Liang et al. (2021). This may be due to the fact that GANs in neuroscience have primarily been applied for data augmentation, often on small, domain-specific datasets, and mainly focused on generating extracted features rather than raw time-series data. As a result, GANs have not been widely utilized as direct neural signal processors or feature extractors.

In this study, we aim to extend the use of GANs beyond data augmentation by incorporating larger-scale EEG recordings—particularly resting-state, task-free data—to train a GAN model for neural data generation. We further explore the utility of the learned representations from its intermediate layers of its discriminator for downstream classification tasks, demonstrating their potential for improving neural signal analysis.

## Methods

### Data

We used the MPI-LEMON dataset (Babayan et al. (2019)), a publicly available resource designed to study mind-body-emotion interactions. This dataset includes resting-state EEG (rs-EEG) recordings from 216 participants, utilizing 61 EEG channels during both eye-closed and eye-open experimental blocks. Data from 13 participants were excluded due to missing event information, different sampling rates, mismatching header files, or insufficient data quality (Babayan et al. (2019)). Each participant contributed a 16-minute EEG recording, resulting in a total of 54.13 hours of rs-EEG data.

**Preprocessing** To preserve the natural structure of the EEG data, we kept preprocessing to a minimum (Delorme (2023)). We first downsampled the EEG signals to 98 Hz. This sampling rate was deliberately chosen as a workaround to remove power line noise (50 Hz) without requiring an additional low-pass or notch filter.

Following the steps outlined in Défossez et al. (2023), we then applied Baseline correction by subtracting the average value of the first 0.5 seconds from each channel. The data was then normalized using Scikit-Learn’s robust scaler, followed by standard scaling. To mitigate the impact of extreme outliers, values exceeding 20 standard deviations were clamped. Data clamping is found to be as effective as more complex artifact rejection methods such as AutoReject (Défossez et al. (2023)).

Finally, EEG signals were high-pass filtered at 0.5 Hz to remove low-frequency drift and were segmented into around 5-second windows (512 time points). In this study, we included eight EEG channels (F1, F2, C1, C2, P1, P2, O1, and O2) to streamline development while maintaining overall generalizability. However, the proposed model is designed to be scalable. Specifically, the capacity of each layer—such as the number of filters in the convolutional layers—is proportional to the number of input channels. This allows the model to be adapted to accommodate and process additional EEG channels as needed.

### Architecture Details

We implemented a Wasserstein Generative Adversarial Network with Gradient Penalty (WGAN-GP) to generate multi-channel EEG data. The model consists of two core components: A generator, responsible for producing synthetic EEG signals, and a discriminator—referred to as a "Critic" in the WGAN framework—which evaluates whether the generated data is real or synthetic.

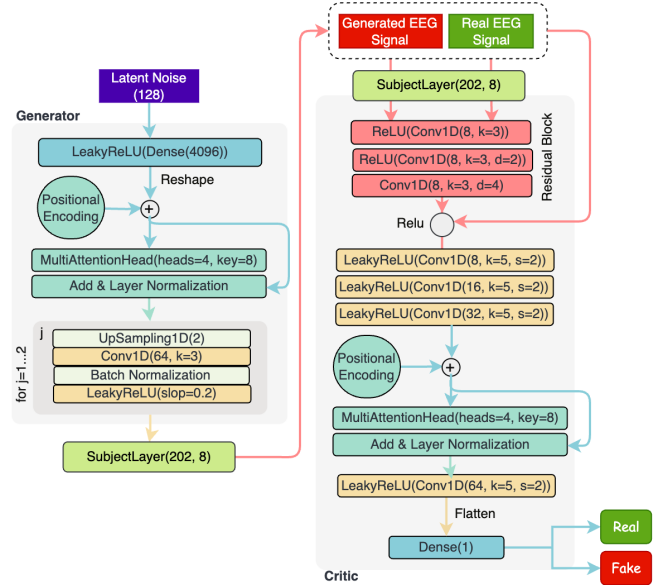


Figure 1: Proposed model’s architecture.

Our architecture follows the Deep Convolutional GAN (DCGAN) (Radford (2015)) framework, incorporating a stack of convolutional layers with upsampling layers in the generator and strided convolutional layers in the Critic (Figure 1). For upsampling, we used linear interpolation, as it has been shown to produce significantly fewer high-frequency artifacts compared to nearest-neighbor upsampling (Hartmann et al. (2018)).

To improve the model’s ability to capture long-range dependencies in EEG signals, we integrated a one-dimensional self-attention mechanism into both the generator and the Critic. This self-attention layer includes: (1) A multi-head attention mechanism applied along the time dimension. (2) a layer normalization module, and, (3) and a learnable positional embedding layer, similar to how they are used in Transformers. Instead of using fixed sinusoidal embeddings (as in Vaswani (2017)), we use trainable positional embeddings for each time step, which are added to the input tensor before feeding the sequence into the multi-head attention block. Our ablation experiment showed that this self-attention layer is essential in model performance in generating realistic and diverse EEG data. All weights in the convolutional and dense layers were initialized using a random normal distribution with a mean of 0 and a standard deviation of 0.02. This initialization has been shown to stabilize GAN training and prevent divergence (Radford (2015)).

To account for individual variability across participants and enhance diversity in the generated EEG signals, we incorporated a participant-specific transformation layer. Inspired by (Défossez et al. (2023)), this layer is applied after the generator produces synthetic data learns a participant-specific transformation matrix  $M \in \mathbb{R}^{D1 \times D1}$  for each participant  $s \in [S]$ . This modification was critical in preventing generator mode

collapse — a scenario where the generator produces only a limited set of examples to deceive the critic. By leveraging this layer, the generator was able to produce more diverse outputs.

## Training

As the name WGAN-GP indicates, in the training of this network we used the Wasserstein loss function.

$$L = \underbrace{\mathbb{E}_{z \sim p(z)} [D(G(z))] - \mathbb{E}_{x \sim p_r} [D(x)]}_{\text{Wasserstein loss}} + \underbrace{\lambda \mathbb{E}_{\hat{x} \sim p_{\hat{x}}} [(\|\nabla_{\hat{x}} D(\hat{x})\|_2 - 1)^2]}_{\text{gradient penalty}}$$

The first term, estimates the distance between the real data distribution and the generated data's distribution using the Wasserstein distance (also known as the Earth Mover's Distance). The second term, known as gradient penalty, ensures that the Critic function remains close to 1-Lipschitz by penalizing deviations of the gradient norm from 1.  $P_{\hat{x}}$  denotes the distribution of points obtained by sampling uniformly along the line segments between real and generated samples.  $\lambda$  is the gradient penalty coefficient. We set the gradient penalty weight to 10.

The generator's loss remains:

$$L_G = \mathbb{E}_{z \sim p(z)} [D(G(z))]$$

since the generator aims to produce samples that maximize  $D(G(z))$  (or equivalently, minimize  $-D(G(z))$ ), thereby reducing the estimated Wasserstein distance between the generated and real distributions.

Both the generator and critic were optimized using the Adam optimizer ( $\beta_1 = 0.5, \beta_2 = 0.9$ ), with an initial learning rate of 0.00094 and a batch size of 128. The learning rate was reduced progressively using an exponential decay schedule with a decay step of 100,000 and a decay rate of 0.90. This gradual reduction in the learning rate was crucial to preventing training instabilities, such as model blow-ups or divergence.

Latent variables  $z$  for the generator were sampled from a normal distribution with the mean and standard deviation of the real data. To ensure the Critic remains well-trained and provides meaningful feedback to the Generator, the Critic was updated twice per each Generator update. Specifically, in each training iteration, two full forward and backward passes were performed on the Critic using both real and generated samples before updating the Generator once.

Data shuffling across batch dimensions was enabled in the Keras fit function, ensuring that each training iteration included segments from different subjects. The model was trained for 2,500 epochs (360,000 steps) on an NVIDIA V100 GPU with mixed precision using CUDA 12.2. The entire model development and training process was implemented using Keras (v3.5.0) with the PyTorch (v2.4.1) backend. The implementation code for this model is available at: <https://github.com/Yeganehfrh/EEGModalNet>

## Evaluation Metrics

To assess the quality of the generated EEG data, we conducted both visual inspections and quantitative comparisons between real and generated signals. We first examined the generated signals in the time and frequency domains to check for realistic waveform structures and spectral properties. Next, we quantified the similarity between real and synthetic data by extracting several statistical and spectral features, including:

**Hjorth parameters** (activity, mobility, complexity) to capture signal variance, frequency composition, and dynamic complexity Hjorth (1970).

**Higher-order statistics**, such as kurtosis and skewness, to analyze the distribution of EEG amplitudes.

**Relative Power spectral features** across standard EEG frequency bands (delta, theta, alpha, beta, gamma) to compare oscillatory activity.

To track how well the model learned the statistical properties of real EEG, we computed the **Fréchet Inception Distance (FID)** Heusel et al. (2017) between the feature distributions for each EEG channel throughout training, measured every 50 epochs. This allowed us to monitor the learning process, identify potential challenges in capturing specific channels' features.

## Classification task: fine-tuning the Critic for a downstream task

To assess whether the representations learned in the intermediate layers of the GAN were useful for a new task, we repurposed the Critic for age group classification. Specifically, we extracted features from the second-to-last layer of the Critic—after the flattening layer but before the final dense layer (which has a dimension of 4096)—and used these learned representations from the EEG data for classification.

Our classification model consisted of two dense layers with 128 and 32 units, both using the ReLU activation function. The final output layer was a dense layer with a Sigmoid activation function. This model received the learned embeddings from the Critic and predicted the corresponding age group class.

For this classification task, we used the same EEG dataset as in the GAN training but resampled it to achieve a balanced age distribution: 50% of participants were above 55 years old, and 50% were below 40 years old. In total, this classification included 130 participants.

For train-test splitting, we used GroupShuffleSplit from Scikit-Learn to prevent data leakage by ensuring that EEG segments from the same participant did not appear in both the training and test sets. The data was split 70% for training and 30% for testing.

We trained the model using binary cross-entropy loss with the Adam optimizer (learning rate = 0.001). Training was conducted for 1000 epochs with a batch size of 256. To evaluate model performance, we used accuracy as the primary metric.

## Results

### Training Statistics

Figure 2 shows the generator and Critic loss curves over 2,500 training epochs. Throughout this process, we also continuously monitored the gradient penalty, the critic's norm, and the critic's prediction of the real and fake data, to ensure stable learning and prevent divergence (Figure 2).

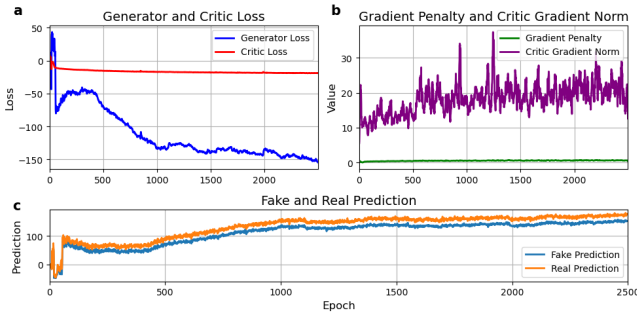


Figure 2: Training Statistics. Each graph shows key metrics tracked over 500 training epochs: (a) Loss curves for the Generator and Critic. (b) Gradient penalty (the L2 norm of the gradient of the Critic with respect to its input data) and Critic gradient norm (the gradient magnitude of the Critic with respect to its weights). (c) The average Critic predictions for real and fake data at each epoch. The Critic consistently assigns higher values to real data, indicating that it continues to learn and has not been fully deceived by the Generator.

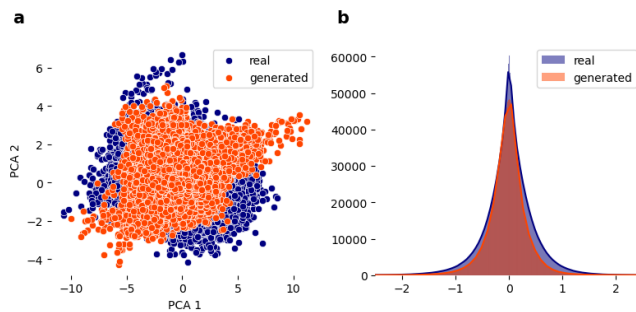


Figure 3: (a) PCA visualization of real (blue) and generated (orange) EEG data in a two-dimensional space, showing the degree of overlap between the distributions. Each point represents an individual EEG segment. (b) Global distribution comparison of real and generated data, aggregated across all EEG channels and time points, illustrating their overall alignment.

### Result 1: The proposed architecture is successful in Generating multi-channels EEG data

Figure 4 presents a visual comparison between real and generated EEG signals, highlighting their average waveforms

and standard deviations in both the time and frequency domains. Despite the model not being explicitly trained on frequency-domain data, the power spectral density (PSD) analysis shows that it successfully captured the spectral characteristics of different EEG channels.

In the time domain, while the generated signals do not perfectly overlap with the real data, they remain within the same dynamic range, demonstrating that the model effectively learned key temporal properties. Also, principal component analysis (PCA) was used to assess the similarity between real and generated data in a lower-dimensional space. By reducing the EEG feature space from 8 channels to 2 principal components, the PCA plot reveals real and generated EEG data exhibit similar distributions in a lower-dimensional space (Figure 3a). Furthermore, the overall distribution of real and synthetic data across all channels (Figure 3b) shows a strong resemblance, further confirming that the model successfully learned the underlying statistical properties of the EEG signals.

To quantify the similarity between real and generated EEG signals, we computed the Fréchet Inception Distance (FID) on features extracted from both the time and frequency domains. Figure 5 illustrates how FID evolves during training across different electrode regions—frontal, central, parietal, and occipital.

As the graph indicates, FID gradually decreases over the course of training, suggesting that the generator becomes increasingly better at producing realistic EEG data. However, a breakdown of FID across different EEG channels reveals that the model learns lower-frequency components more effectively than higher-frequency components. It might be because those signals naturally have higher energy, making them easier for the network to learn. Additionally, the generator struggles more with frontal EEG channels compared to posterior regions, particularly in the higher gamma frequency range. This suggests that higher-order cognitive activity patterns, which are often more complex in frontal regions, are more challenging for the model to replicate.

### Result 2: The proposed Critic learns useful representation, making it reusable for a downstream tasks (age group classification in this case)

To assess whether the Critic's learned representations are useful for a new task, we evaluated its performance on age group classification. Figure 6a shows the training and validation accuracy of the fine-tuned Critic, with validation accuracy reaching 61%. This is significantly higher than the baseline accuracy observed when evaluating the classifier on shuffled labels (Figure 6c), confirming that the Critic has captured meaningful EEG features.

These results indicate that, in the process of discriminating between real and generated EEG data, the Critic has learned transferable representations of EEG structure that can be reused for an entirely new classification task. This finding highlights the potential of unsupervised representation learn-

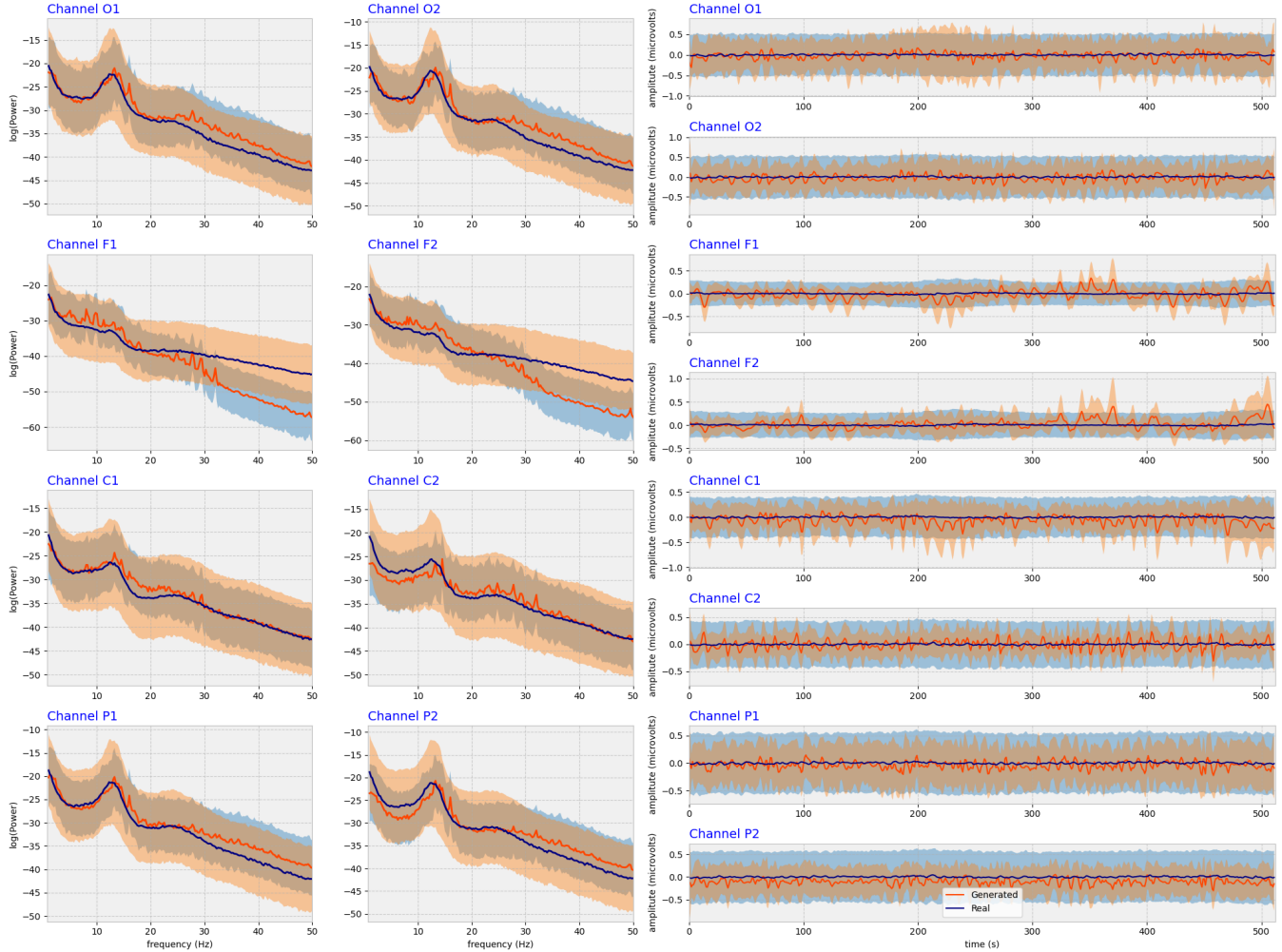


Figure 4: Visual inspection of generated and real data in the frequency and time domains across eight different EEG channels. The power spectral density (PSD) and time-series data are averaged over segments (batch dimension), with the shaded regions indicating the standard deviation. In all subplots, the blue line represents the real data, while the orange line shows the generated data.

ing using GAN-based architecture in EEG analysis, reducing the need for extensive feature engineering.

## Discussion and Conclusion

In this study, we implemented a Wasserstein Generative Adversarial Network with Gradient Penalty (WGAN-GP) to generate multi-channel EEG data and evaluated the quality of the synthesized signals using both visual inspection and feature-based quantitative measures. Our results demonstrate that the model successfully learned key statistical and spectral characteristics of EEG signals, as evidenced by the decreasing Fréchet Inception Distance (FID) over training epochs. However, we observed that the generator struggled more with replicating high-frequency components (gamma band) in the frontal region, suggesting that these aspects of neural data are more complex to capture.

Beyond data generation, we assessed the transferability of

the learned representations by fine-tuning the Critic for age group classification. The model achieved a validation accuracy of 61%, significantly outperforming a shuffled-label baseline, indicating that the GAN's discriminator had effectively learned useful EEG features that could generalize to new tasks. This underscores the potential of unsupervised representation learning for reducing reliance on extensive feature engineering in EEG analysis.

**Limitations** Despite the promising results, our approach has several limitations. First, the training data was derived from a single dataset (LEMON) and limited to eight selected EEG channels, which may restrict the model's ability to generalize to datasets with different recording conditions or additional EEG channels distributed across the scalp.

Second, while we demonstrated that GAN-derived features are transferable to a simple classification task (age prediction),

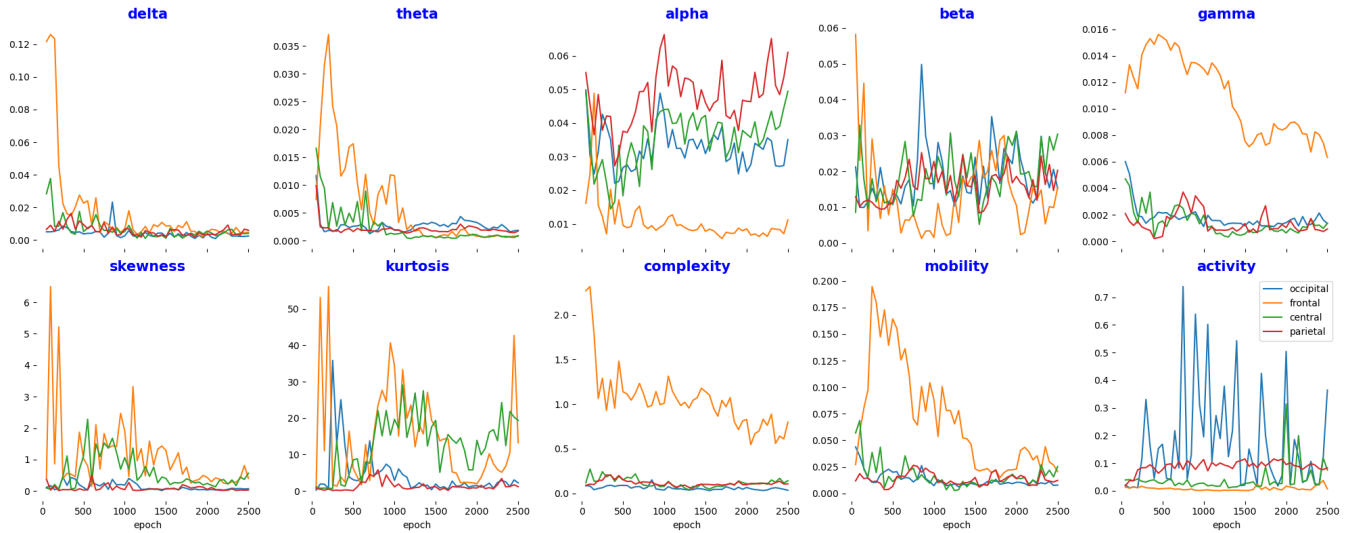


Figure 5: Fréchet Inception Distance (FID) over training epochs. The upper row shows the FID between real and generated data for spectral features, measured as power within standard EEG frequency bands (delta, theta, alpha, beta, gamma) across different electrode regions. The lower row presents the FID evolution for manually extracted time-domain features, including Hjorth parameters (complexity, mobility, activity), skewness, and kurtosis. A decreasing FID over epochs indicates that the generated data increasingly resembles real EEG signals, though differences remain across frequency bands and electrode locations.

their utility in more complex neurocognitive tasks or clinical applications remains unexplored. Additionally, when using the Critic as a feature extractor, we tested it on the same dataset it was trained on, albeit for a different task. Future studies should evaluate the generalizability of these learned representations on entirely new EEG datasets to assess their robustness. Third, we have yet to perform benchmarking or compare our model's performance against existing GAN-based approaches for EEG timeseries generation. Such comparisons would provide deeper insights into our model's strengths and potential areas for improvement.

#### Future Directions

Moving forward, we aim to:

- Expand training data by incorporating larger, more diverse EEG datasets, including task-related and clinical recordings to improve generalizability.
- Enhance high-frequency EEG generation, potentially by implementing spectral-aware loss functions (e.g., spectral regularization) or integrating architectures that incorporate spatial EEG channel embeddings.
- Explore broader applications of the learned representations in tasks such as cognitive state decoding and neurological disorder detection.
- Improve model interpretability by analyzing the latent representations learned by the GAN. Specifically, we plan to investigate which EEG channels contribute most to the learned features, as well as the attention weights in downstream classification tasks. This analysis will help identify

the most influential features in the model's internal representations.

Overall, this study highlights the potential of GAN-based unsupervised learning for EEG data synthesis and representation learning, paving the way for future advancements in data-efficient deep learning applications in neuroscience.

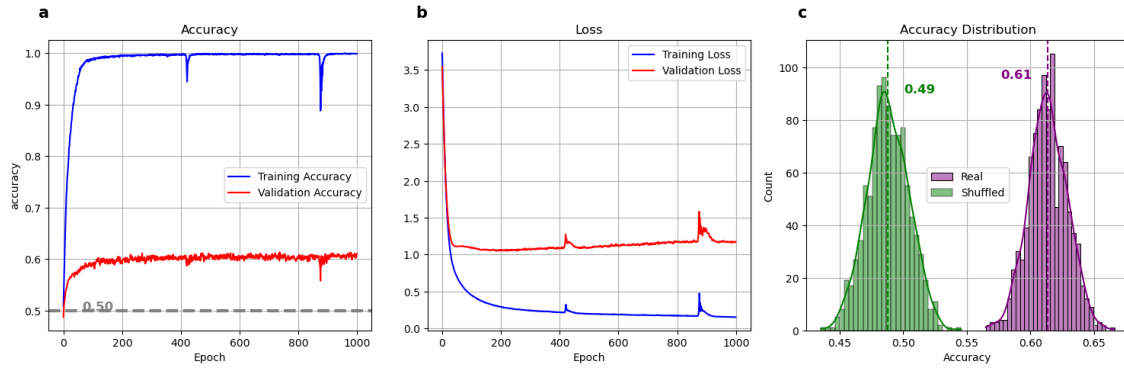


Figure 6: Performance of the fine-tuned model in the age group classification task. (a) Training and validation accuracy over 1000 epochs, with horizontal dashed lines indicating the equal prevalence of each class at 50%. (b) Training and validation loss progression throughout the training process. (c) Accuracy distribution of the model when evaluated on real versus shuffled labels, with vertical dashed lines marking the mean accuracy for each distribution.

## References

- Babayan, A., Erbey, M., Kumral, D., Reinelt, J. D., Reiter, A. M., Röbbing, J., ... others (2019). A mind-brain-body dataset of mri, eeg, cognition, emotion, and peripheral physiology in young and old adults. *Scientific data*, 6(1), 1–21.
- Botvinik-Nezer, R., Holzmeister, F., Camerer, C. F., Dreber, A., Huber, J., Johannesson, M., ... others (2020). Variability in the analysis of a single neuroimaging dataset by many teams. *Nature*, 582(7810), 84–88.
- Défossez, A., Caucheteux, C., Rapin, J., Kabeli, O., & King, J.-R. (2023). Decoding speech perception from non-invasive brain recordings. *Nature Machine Intelligence*, 5(10), 1097–1107.
- Delorme, A. (2023). Eeg is better left alone. *Scientific reports*, 13(1), 2372.
- Fahimi, F., Dosen, S., Ang, K. K., Mrachacz-Kersting, N., & Guan, C. (2020). Generative adversarial networks-based data augmentation for brain-computer interface. *IEEE transactions on neural networks and learning systems*, 32(9), 4039–4051.
- Goodfellow, I., Pouget-Abadie, J., Mirza, M., Xu, B., Warde-Farley, D., Ozair, S., ... Bengio, Y. (2014). Generative adversarial nets. *Advances in neural information processing systems*, 27.
- Hartmann, K. G., Schirrmester, R. T., & Ball, T. (2018). Eeg-gan: Generative adversarial networks for electroencephalographic (eeg) brain signals. *arXiv preprint arXiv:1806.01875*.
- Heusel, M., Ramsauer, H., Unterthiner, T., Nessler, B., & Hochreiter, S. (2017). Gans trained by a two time-scale update rule converge to a local nash equilibrium. *Advances in neural information processing systems*, 30.
- Hjorth, B. (1970). Eeg analysis based on time domain properties. *Electroencephalography and clinical neurophysiology*, 29(3), 306–310.
- Ho, J., Jain, A., & Abbeel, P. (2020). Denoising diffusion probabilistic models. *Advances in neural information processing systems*, 33, 6840–6851.
- Kingma, D. P. (2013). Auto-encoding variational bayes. *arXiv preprint arXiv:1312.6114*.
- Liang, Z., Zhou, R., Zhang, L., Li, L., Huang, G., Zhang, Z., & Ishii, S. (2021). Eegfusenet: Hybrid unsupervised deep feature characterization and fusion for high-dimensional eeg with an application to emotion recognition. *IEEE Transactions on Neural Systems and Rehabilitation Engineering*, 29, 1913–1925.
- Murphy, K. P. (2022). *Probabilistic machine learning: an introduction*. MIT press.
- Pan, B., & Zheng, W. (2021). Emotion recognition based on eeg using generative adversarial nets and convolutional neural network. *computational and Mathematical Methods in Medicine*, 2021(1), 2520394.
- Pascual, D., Amirshahi, A., Aminifar, A., Atienza, D., Rylvlin, P., & Wattenhofer, R. (2020). Epilepsygan: Synthetic epileptic brain activities with privacy preservation. *IEEE Transactions on Biomedical Engineering*, 68(8), 2435–2446.
- Radford, A. (2015). Unsupervised representation learning with deep convolutional generative adversarial networks. *arXiv preprint arXiv:1511.06434*.
- Robbins, K. A., Touryan, J., Mullen, T., Kothe, C., & Bigdely-Shamlo, N. (2020). How sensitive are eeg results to pre-processing methods: a benchmarking study. *IEEE transactions on neural systems and rehabilitation engineering*, 28(5), 1081–1090.
- Vaswani, A. (2017). Attention is all you need. *Advances in Neural Information Processing Systems*.
- Wang, J., Zhao, S., Luo, Z., Zhou, Y., Jiang, H., Li, S., ... Pan, G. (2024). Cbramod: A criss-cross brain foundation model for eeg decoding. *arXiv preprint arXiv:2412.07236*.